Tunable Three-Body Interactions in Driven Two-Component Bose-Einstein Condensates

A. Hammond, L. Lavoine, and T. Bourdel*
Université Paris-Saclay, Institut d'Optique Graduate School, CNRS, Laboratoire Charles Fabry, 91127 Palaiseau, France

(Received 29 November 2021; revised 21 January 2022; accepted 7 February 2022; published 23 February 2022)

We propose and demonstrate the appearance of an effective attractive three-body interaction in coherently driven two-component Bose-Einstein condensates. It originates from the spinor degree of freedom that is affected by a two-body mean-field shift of the driven transition frequency. Importantly, its strength can be controlled with the Rabi-coupling strength and it does not come with additional losses. In the experiment, the three-body interactions are adjusted to play a predominant role in the equation of state of a cigar-shaped trapped condensate. This is confirmed through two striking observations: a downshift of the radial breathing mode frequency and the radial collapses for positive values of the dressed-state scattering length.

DOI: 10.1103/PhysRevLett.128.083401

Thanks to their extreme diluteness, particles in ultracold gases dominantly interact pairwise. At low temperatures, the thermal de Broglie wavelength is larger than the range of the Van der Waals potential R_e, and the two-body interaction can accurately be replaced by a contact potential [1]. Moreover, the only parameter characterizing the interaction, i.e., the scattering length a, can be tuned via scattering resonances [2]. Thanks to these properties, ultracold gases are ideal candidates to quantitatively explore quantum many-body physics with pairwise interactions [3]. For example, the superfluid to Mott transition [4] or the BEC-BCS crossover [5–9] have been studied.

Although three-body interactions are usually a small correction compared to two-body interactions in dilute gases, their theoretical consideration has a long history [10–12]. They lead to interesting nonlinear dynamics [13–21] and to the appearance of droplets [22,23]. At low temperatures, a three-body interaction is characterized by a scattering hypervolume D [24]. D is a complex number whose real part is associated with an energy shift and its imaginary part with three-body losses. Enhancement of three-body interactions, i.e., of the real part of D, is expected close to resonances due to energy coincidence with weakly bound three-body states [22,24–28]. Unfortunately, typical interatomic interaction potentials possess numerous deeply bound two-body states and the enhancement of the real part of D comes together with a concomitant increase of its imaginary part due to three-body recombination toward these states [29]. For example, three-body Efimov resonances have been experimentally observed through the enhancement of losses [30,31]. In optical lattices, the engineering of three-body interactions was proposed via strong three-body losses and quantum Zeno effect [32,33] or via a coherent coupling between two spin states [34].

Alternatively, an effective three-body interaction can be induced through a density dependant two-body coupling strength. This method requires an additional degree of freedom that rapidly adjusts to the local density and can be adiabatically eliminated. For a condensate in quasi-one-dimensional (1D) or quasi-2D geometries, the wave function in the confined direction provides this additional degree of freedom [35–37]; its size slightly increases (decreases) for repulsive (attractive) two-body interactions. This effect leads to an effective attractive three-body coupling constant $g_3 \propto -a^2$ in the equation of state in the reduced geometry. Note that it is a perturbative expansion, valid when the three-body energy is a small correction to the two-body energy. Manifestations of these three-body interactions were observed in frequency shifts of breathing oscillations in a quasi-2D geometry [37] and in the breaking of integrability in quasi-1D gases [36].

In this Letter, we demonstrate that the additional spinor degree of freedom in coherently driven two-component condensates can similarly induce effective three-body interactions after its adiabatic elimination. The method crucially relies on two facts: first, the scattering lengths in the dressed states depend on their spin composition [38,39]; second, the spin composition is affected by density-induced mean-field shifts of the driven transition [40,41]. In contrast to condensates in a reduced dimension, the two parameters in driven two-component condensates (the detuning frequency $\delta/2\pi$ and the Rabi-coupling frequency $\Omega/2\pi$) allow the independent control of the two-body and three-body coupling constants. The two-body interactions can thus be reduced such that the three-body interactions prevail in the equation of states. In addition, these three-body interactions appear at the mean-field level and can be made significantly larger in magnitude than the recently studied beyond mean-field three-body effects [42,43].

Experimentally, we study two consequences of the effective attractive three-body interactions that appear in the lowest energy dressed state of a driven two-component

^{39}K condensate. First, the radial breathing mode frequency of an elongated condensate, which is usually independent of the two-body interaction, exhibits a downshift. Second, we measure the detuning threshold for radial collapse as a function of Ω. We find that the condensate collapses despite a positive scattering length due to the attractive three-body interactions. Importantly, we detect no increase of losses associated with the introduction of the coherent coupling that enables the tuning of the two-body and three-body interactions.

Let us consider a Bose gas in a volume V consisting of N atoms of mass m with two coupled internal states, $\sigma = \uparrow, \downarrow$. For simplicity, we work with symmetric interactions, $g_{\uparrow\uparrow} = g_{\downarrow\downarrow} = g$, and we define $\bar{g} = (g_{\uparrow\uparrow} - g_{\uparrow\downarrow})/2$ (with $g_{\sigma\sigma'} = 4\pi\hbar^2 a_{\sigma\sigma'}/m$ and $\hbar$ the reduced Planck constant). In a homogeneous system with density n, the mean-field energy for a condensate in the spinor state $(\phi_\uparrow, \phi_\downarrow)$ reads

$$\frac{E_{\mathrm{MF}}}{V} = -\frac{\hbar\Omega}{2}(\phi_\uparrow^*\phi_\downarrow + \phi_\downarrow^*\phi_\uparrow) + \frac{\hbar\delta}{2}(|\phi_\uparrow|^2 - |\phi_\downarrow|^2) + \sum_{\sigma\sigma'}\frac{g_{\sigma\sigma'}}{2}|\phi_\sigma|^2|\phi_{\sigma'}|^2.$$

The ground state is found upon minimization of the energy with respect to the internal state. The first term fixes the relative phase of the spinor that we can thus write $(\phi_\uparrow, \phi_\downarrow) = \sqrt{n}[\sin(\theta/2), \cos(\theta/2)]$. The energy is

$$\frac{E_{\mathrm{MF}}}{N} = -\frac{\hbar\Omega}{2}\sin(\theta) - \frac{\hbar\delta}{2}\cos(\theta) + \frac{gn}{2} - \frac{\bar{g}n}{2}\sin^2(\theta) \quad (1)$$

with $\theta \in [0, \pi]$ found upon minimization. Up to first order in the ratio $\gamma = [(\bar{g}n)/(\hbar\Omega)]$, which compares the differential mean-field shift to the Rabi frequency, we find

$$\theta \approx \theta_0 - 2\gamma\frac{\delta/\Omega}{(1+\delta^2/\Omega^2)^{3/2}} \quad \text{with} \quad \mathrm{cotan}(\theta_0) = \frac{\delta}{\Omega}. \quad (2)$$

In the absence of interaction ($\gamma = 0$), $\theta = \theta_0$ corresponds to a condensate in the single particle eigenstate of lowest energy $|-\rangle = \sin(\theta_0/2)|\uparrow\rangle + \cos(\theta_0/2)|\downarrow\rangle$. In the presence of interaction, γ is the key parameter controlling the modification of the internal state away from $|-\rangle$. It results in the following mean-field energy per particle:

$$\frac{E_{\mathrm{MF}}}{N} \approx \epsilon_- + g_2\frac{n}{2} + g_3\frac{n^2}{3} \quad (3)$$

$$\text{with} \quad g_2 = g - \frac{\bar{g}}{1+\delta^2/\Omega^2} \quad (4)$$

$$\text{and} \quad g_3 = -\frac{3\bar{g}^2}{\hbar\Omega}\frac{\delta^2/\Omega^2}{(1+\delta^2/\Omega^2)^{5/2}}. \quad (5)$$

The first term in Eq. (3) is the single particle eigenenergy $\epsilon_- = -\hbar\sqrt{\Omega^2+\delta^2}/2$ of the $|-\rangle$ state. $g_2 = 4\pi\hbar^2 a_{--}/m$ corresponds to the two-body coupling constant for atoms in $|-\rangle$ [39]. It is solely determined by the ratio δ/Ω [see Fig. 2(b)]. g_3 is an attractive three-body coupling constant appearing due to the mean-field–induced change in θ [Eq. (2)]. It is zero both for large absolute value of δ/Ω when the two states are uncoupled and for $\delta = 0$ as the energy [Eq. (1)] is then always minimal for $\theta = \theta_0 = \pi/2$.

Interestingly, g_3 can be independently controlled from g_2 through the value of Ω. Nonetheless, there are some limitations. First, Ω can not be made arbitrarily small as the adiabatic following of the dressed state requires $\dot{\gamma} \ll \Omega$ when the density varies in time. Second, the energy expansion in powers of the density [Eq. (3)], i.e., the three-body approximation, is only valid for $\gamma \ll 1$. This second condition is more restrictive for our experimental conditions (see below) and taking $\gamma \approx 1$ or $\hbar\Omega \approx \bar{g}n$, we find that the maximum absolute value of the three-body energy per particle $g_3 n^2/3$ amounts to a significant fraction of $\bar{g}n$. It can thus compete with the two-body energy $g_2 n/2$. In the limit $\gamma \gg 1$ and $\bar{g}n \gg \hbar|\delta|$, $\theta \approx \pi/2$ and the energy [Eq. (1)] recovers a two-body behavior with $g_2 = (g - \bar{g})$.

We now turn to the experimental observation of the three-body interactions. We work with the second and third lowest Zeeman states of the lowest manifold of ^{39}K, namely $|\uparrow\rangle = |F = 1, m_F = -1\rangle$ and $|\downarrow\rangle = |F = 1, m_F = 0\rangle$. At a magnetic field of 54.690(1) G, the three relevant scattering lengths are $a_{\uparrow\uparrow} = 37.9\, a_0$, $a_{\downarrow\downarrow} = 36.9\ a_0$ [44], and $a_{\uparrow\downarrow} = -54.2\ a_0$, where a_0 is the atomic Bohr radius [45]. With these specific parameters, the scattering length a_{--} has a minimum $-8.4\ a_0$ for $\delta \approx 0$ and zero crossings at $\delta/\Omega \approx \pm 0.47$ (see Fig. 3). Because of an experimental rms magnetic field noise of 0.8(2) mG corresponding to 0.56 (14) kHz, we choose to work with $\Omega/2\pi \geq 7$ kHz in order to keep a good control of the parameter δ/Ω. For this value of Ω and $\delta/\Omega \approx 0.8$, the maximum absolute value of the three-body coupling constant is $|g_3|/\hbar = 3 \times 10^{-38}\ \mathrm{m^6\,s^{-1}}$. This value is larger by a factor of $\sim$100 compared to the dominant three-body loss coefficient $K_3^{\downarrow\downarrow\downarrow}/6 \approx 3 \times 10^{-40}\ \mathrm{m^6\,s^{-1}}$ in our potassium mixtures [46]. The hypervolume D for our parameters is thus essentially real with $|\Re(D)| \gg \Im(D)$. $|g_3|$ is also larger than the three-body coupling constant emerging from beyond mean-field effects [43] by a factor of $\sim$50 and the latter is neglected in the present work.

The experiment starts with a quasipure Bose-Einstein condensate with $\sim 1.4 \times 10^5$ atoms in state $|\uparrow\rangle$ in a cigar-shaped trap with frequencies $(\omega_\perp, \omega_\parallel)/2\pi = (300, 16.4)$ Hz. The condensate in the ground state is then prepared in an adiabatic passage, in which the rf detuning is swept from 7.5 Ω to its final value δ. Its shape and duration of 0.4 ms are chosen in order to be adiabatic with respect to the internal-state dynamics but it is short as compared to $2\pi/\omega_\perp$. As a

consequence, the rf sweep is equivalent to a quench of the interaction parameters and it induces some dynamics of the cloud. In the longitudinal direction, the evolution is slow and we neglect it on the 15 ms timescale of our experiment [47]. We focus our analysis on the radial dynamics of the condensate in its central part where the 1D density n_{1D} is approximately constant.

In a first series of experiments, we chose parameters ($\Omega/2\pi = 25.4$ kHz and $\delta/\Omega > 0.8$) for which, we observe small amplitude breathing oscillations of the radial size (see inset in Fig. 1) [48]. On the 15 ms timescale of the experiment, we find that the atom number is reduced by a maximum of 20%. Interestingly, we measure a reduction of the breathing mode frequency when δ/Ω is decreased from 1.4 to 0.8 (see Fig. 1), whereas, in the absence of three-body interaction, it is expected to be constant and equal to $2\omega_\perp$ independently of the two-body contact interaction due to a hidden symmetry of the Hamiltonian under scale transformation [49–51].

Let us now compare the measured frequencies to theoretical expectations for a condensate for which the equation of state is given by Eq. (3). In a variational and scaling approach [52,53], the frequency of small [48] breathing oscillations writes

$$\omega_b = 2\omega_\perp \sqrt{1 + E_3/E_{\rm pot}}, \tag{6}$$

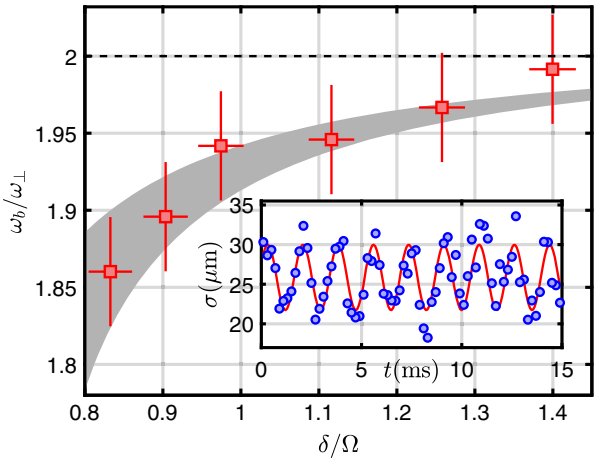

FIG. 1. Breathing frequency at Rabi frequency $\Omega = 25.4$ kHz as a function of the detuning δ/Ω. The points correspond to the experimental data. The vertical error bars correspond to a 1.5% uncertainty in the measured frequency. The horizontal error bars are linked to our 0.8(2) mG magnetic field fluctuations. The shaded area corresponds to the theoretical estimates for 2.3×10^9 m^{-1} $< n_{1D} < 2.65 \times 10^9$ m^{-1} taking into account the uncertainty in the value of n_{1D} due to experimental fluctuations, losses, and uncertainty in the detection efficiency. Inset: radial breathing oscillations for $\delta/\Omega = 0.9$. The rms size σ of the gas is measured as a function of the wait time t after 9.7 ms of free expansion, including an initial 0.4 ms rf sweep back to $\delta = 7.5\ \Omega$.

where $E_3 < 0$ and $E_{\rm pot}$ are the three-body and potential energy in the equilibrium state. We calculate these two quantities from imaginary time evolution of a 2D extended Gross-Pitaevskii equation [54] and deduce the value of the breathing mode frequency (see Fig. 1). Within the experimental error bars, we find a perfect agreement with the measured values and we thus attribute the breathing mode frequency downshift to the attractive three-body interactions. Note that in the explored range, decreasing δ/Ω corresponds both to a decrease of g_2 and to an increase of $|g_3|$.

By lowering further the value of δ/Ω, we observe large losses that rapidly occur around ~1 ms after the beginning of the rf sweep, i.e., when the condensate has shrunk to a high density. In order to study this behavior, we wait 3 ms after the sweep and plot the remaining central 1D density as a function of δ/Ω for two values of Ω [see Fig. 2(a)]. At large values of $|\delta/\Omega|$, there are few losses and the 1D density is close to the initial one. On the contrary, for low values of $|\delta/\Omega|$, the 1D density is observed to be reduced by a factor of ~3. Interestingly, the losses appear sharply as a function of $|\delta/\Omega|$ and we interpret this behavior as originating from a radial collapse of the cloud, which is certainly expected for $\delta/\Omega \approx 0$ where the minimum scattering length is $a_{--} = -8.4\ a_0 < 0$. In the following, we do not try to precisely understand the collapse dynamics, including the role of losses, but rather focus our analysis on the threshold values δ_c/Ω below which a collapse occurs.

The collapse thresholds δ_c/Ω are plotted as a function of Ω in Fig. 3 and are found to be larger for lower values of Ω. Such a behavior reveals the role of three-body interactions in the radial collapse as g_2 solely depends on the ratio δ/Ω. Moreover, for $\Omega/2\pi < 20$ kHz the collapse is observed for $\delta/\Omega > 0.47$, which corresponds to a positive scattering

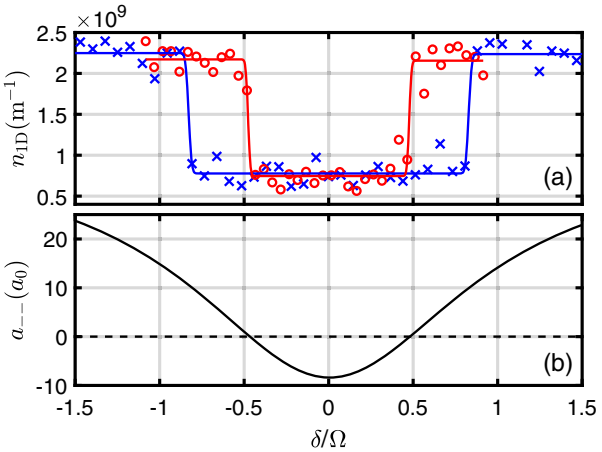

FIG. 2. (a) Remaining 1D density as a function of the final detuning δ/Ω. $\times$: $\Omega/2\pi = 7.6$ kHz, $\circ$: $\Omega/2\pi = 29.8$ kHz. The curves are fits with the function $n_{\rm coll} + (n_{1D} - n_{\rm coll})\,{\rm erf}[(|\delta| - \delta_c)/(W\Omega)]$, where $n_{\rm coll}$, n_{1D}, W, and δ_c are free parameters. (b) Scattering length a_{--} as a function of δ/Ω.

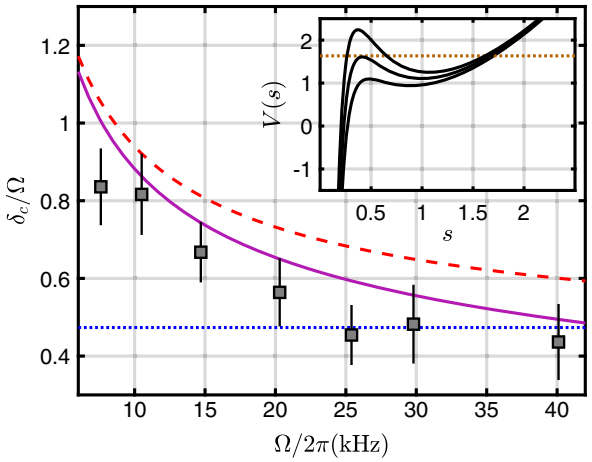

FIG. 3. Collapse threshold as a function of the Rabi frequency $\Omega/2\pi$. The squares are the experimental data. The dotted blue line at $\delta/\Omega = 0.47$ corresponds to $a_{--} = 0$. The solid purple (dashed red) line corresponds to the theoretical prediction taking into account the mean-field effect on the internal state with (and without) the renormalization of the two-body interaction (see text). Inset: Effective potentials V for $\Omega/2\pi = 30$ kHz for $\delta/\Omega = 0.54$ (top curve), $\delta/\Omega = 0.49 = \delta_c/\Omega$ (middle curve), $\delta/\Omega = 0.44$ (bottom curve). The dotted line is the initial energy for the middle curve corresponding to $s(0) = 1.7$.

length a_{--}, i.e., repulsive two-body interactions [see Fig. 2(b)]. As an example, for $\Omega = 7.6$ kHz, $\delta_c/\Omega = 0.82(5)$ corresponds to $a_{--} \approx 10\ a_0$ (see Fig. 2).

In order to quantitatively interpret our findings, we develop a model that assumes a Gaussian radial density profile at all times t with a rms radius $\sqrt{\langle r^2 \rangle} = s(t) a_{\mathrm{ho}}$, where $a_{\mathrm{ho}} = \sqrt{\hbar/m\omega_\perp}$ corresponds to the noninteracting equilibrium rms radius. The energy density is then calculated upon local minimization with respect to internal state according to Eq. (1). After integration over the radial profile, the total energy E can then be cast as

$$\frac{E}{N\hbar\omega_\perp} = \frac{\epsilon_-}{\hbar\omega_\perp} + \frac{\dot{s}^2}{2} + \underbrace{\frac{s^2}{2} + \frac{1}{2s^2} + \frac{E_{\mathrm{int}}(s)}{N\hbar\omega_\perp}}_{V(s)}, \tag{7}$$

where the terms on the right-hand side respectively correspond to the single particle internal energy, the kinetic energy associated to particle flow, the harmonic potential energy, the zero-point kinetic energy [55], and the interaction energy [57]. In the limit $\gamma \ll 1$, the latter can be calculated from Eq. (3) and amounts to $[E_{\mathrm{int}}(s)/N] = [(g_2 n_{1\mathrm{D}})/(4\pi a_{\mathrm{oh}}^2 s^2)] + [(g_3 n_{1\mathrm{D}}^2)/(12\pi^2 a_{\mathrm{oh}}^4 s^4)]$. Since we only see important losses when the collapse has occurred, we do not include a loss term in the initial dynamics. In our framework, the latter reduces to the one of a classical particle in an effective potential $V(s)$ given by the three last terms in Eq. (7).

Since $\gamma \sim 1$ for some of our parameters, we rely on numerical calculations of $E_{\mathrm{int}}(s)$ [57]. Typical effective potentials $V(s)$ close to the collapse threshold are plotted in the inset of Fig. 3. They exhibit a local maximum for low value of s that may be overcome or not depending on the initial energy, which is given by the initial rms size of the cloud. The latter is numerically computed [54] to 1.1 μm corresponding to $s(0) = 1.7$. For each value of Ω, we find the collapse threshold δ_c/Ω for which the local maximum of $V(s)$ is equal to $V[s(0)]$. This model for the collapse threshold (dashed curve in Fig. 3) captures the trend of the threshold values δ_c/Ω but slightly overestimates them. As an improvement to our model, we take into account the main beyond mean-field two-body correction to a_{--} (see the supplemental material of [43]). A better match to the experimental data is then obtained (solid line in Fig. 3), strengthening our interpretation [58].

To conclude, we have shown that a Rabi-coupled two component Bose-Einstein condensate with different scattering lengths offers a way to induce an attractive three-body term in the equation of state. The latter appears, at the mean-field level, because of a density-dependent detuning of the drive. It is tunable through the Rabi-coupling strength and can be adjusted to play an important role in the condensate dynamics. The attractive three-body energy can also be made much larger than the energy associated with the three-body loss rate. Experimentally, we observe two striking consequences of the attractive three-body term: a shift of the radial breathing mode frequency and radial collapses despite repulsive two-body couplings $g_2 > 0$. Our findings can be easily generalized to the asymmetric case ($a_{\uparrow\uparrow} \neq a_{\downarrow\downarrow}$). In this case, there is experimentally much more freedom in the choice of the atomic species, of the specific spin states, and of the magnetic field such that optimal conditions, i.e., a large three-body coupling constant and a low three-body loss rate, could be found.

The presence of three-body interactions modifies the thermodynamical properties of quantum Bose gases with consequences such as a change of the condensation temperature [59] or frequency shifts of low energy excitation modes [19]. Stronger excitations such as vortices [60], dark solitons [15], or dispersive shock waves [17,18] will also have modified properties. In particular, the additional nonlinear term breaks the integrability in the soliton dynamics [61].

Finally, we discuss the possibility of creating a repulsive three-body term with a condensate in an internal state that maximizes the energy [Eq. (1)] [62]. In this case $\theta \in [-\pi, 0]$ and g_3 is positive. Unfortunately, a condensate in such a state suffers from large two-body losses [39]. The two-body loss rate is $\Gamma \sim \hbar n \bar{a}^2/m l_\Omega$, where $\bar{a} = (a_{\uparrow\uparrow} - a_{\uparrow\downarrow})/2$ and $l_\Omega = \sqrt{\hbar/m\Omega}$ is a length scale associated with Ω. Reducing the value of Ω would open a window where the repulsive three-body energy $E_3 \propto g_3 n^2$ could dominate over the two-body loss rate for $E_3/\hbar\Gamma \propto n l_\Omega^3 \gg 1$.

Repulsive three-body interactions produced in this manner would offer an alternative way to create gaseous droplets compared to beyond mean-field effects [63–68]. Quantum droplets [69] and few-body bound states [70,71] were recently discussed in the case of 1D bosons with repulsive three-body interactions. With such nonlinear interactions, Bose-Einstein condensation in a harmonic trap is also predicted to become first order [72].

We thank D. Clément, D. Petrov, S. Kokkelmans, L. Tarruell, C. Westbrook, and W. Zwerger for useful discussions. This research has been supported by CNRS, Ministère de l'Enseignement Supérieur et de la Recherche, Labex PALM, Région Ile-de-France in the framework of Domaine d'Intérêt Majeur Sirteq, Paris-Saclay in the framework of IQUPS, ANR Droplets (19-CE30-0003), and Simons Foundation (Grant No. 563916: localization of waves).

*Corresponding author.
thomas.bourdel@institutoptique.fr

[1] L. Pitaevskii and S. Stringari, *Bose-Einstein Condensation and Superfluidity* (Oxford University Press, New York, 2003).
[2] C. Chin, R. Grimm, P. Julienne, and E. Tiesinga, Feshbach resonances in ultracold gases, Rev. Mod. Phys. **82**, 1225 (2010).
[3] I. Bloch, J. Dalibard, and W. Zwerger, Many-body physics with ultracold gases, Rev. Mod. Phys. **80**, 885 (2008).
[4] M. Greiner, O. Mandel, T. Esslinger, T. W. Hänsch, and I. Bloch, Quantum phase transition from a superfluid to a Mott insulator in a gas of ultracold atoms, Nature (London) **415**, 39 (2002).
[5] C. A. Regal, M. Greiner, and D. S. Jin, Observation of Resonance Condensation of Fermionic Atom Pairs, Phys. Rev. Lett. **92**, 040403 (2004).
[6] M. W. Zwierlein, C. A. Stan, C. H. Schunck, S. M. F. Raupach, A. J. Kerman, and W. Ketterle, Condensation of Pairs of Fermionic Atoms near a Feshbach Resonance, Phys. Rev. Lett. **92**, 120403 (2004).
[7] M. Bartenstein, A. Altmeyer, S. Riedl, S. Jochim, C. Chin, J. Hecker Denschlag, and R. Grimm, Crossover from a Molecular Bose-Einstein Condensate to a Degenerate Fermi Gas, Phys. Rev. Lett. **92**, 120401 (2004).
[8] T. Bourdel, L. Khaykovich, J. Cubizolles, J. Zhang, F. Chevy, M. Teichmann, L. Tarruell, S. J. J. M. F. Kokkelmans, and C. Salomon, Experimental Study of the BEC-BCS Crossover Region in Lithium 6, Phys. Rev. Lett. **93**, 050401 (2004).
[9] W. Zwerger, Strongly Interacting fermi gases, *Proceedings of the International School of Physics "Enrico Fermi"*, edited by M. Inguscio, W. Ketterle, S. Stringari, and G. Roati (IOS Press, Amsterdam, SIF Bologna, 2016), pp. 63.
[10] T. T. Wu, Ground state of a Bose system of hard spheres, Phys. Rev. **115**, 1390 (1959).
[11] T. Köhler, Three-Body Problem in a Dilute Bose-Einstein Condensate, Phys. Rev. Lett. **89**, 210404 (2002).
[12] H. W. Hammer, A. Nogga, and A. Schwenk, Colloquium: Three-body forces: From cold atoms to nuclei, Rev. Mod. Phys. **85**, 197 (2013).
[13] A. Gammal, T. Frederico, L. Tomio, and P. Chomaz, Atomic Bose-Einstein condensation with three-body interactions and collective excitations, J. Phys. B **33**, 4053 (2000).
[14] A. Gammal, T. Frederico, L. Tomio, and F. K. Abdullaev, Stability analysis of the D-dimensional nonlinear Schrödinger equation with trap and two- and three-body interactions, Phys. Lett. A **267**, 305 (2000).
[15] A. M. Kamchatnov and M. Salerno, Dark soliton oscillations in Bose-Einstein condensates with multi-body interactions, J. Phys. B **42**,185303 (2009).
[16] V. R. Kumar, R. Radha, and M. Wadati, Phase engineering and solitons of Bose–Einstein condensates with two- and three-body interactions, J. Phys. Soc. Jpn. **79**, 074005 (2010).
[17] M. Crosta, S. Trillo, and A. Fratalocchi, Crossover dynamics of dispersive shocks in Bose-Einstein condensates characterized by two and three-body interactions, Phys. Rev. A **85**, 043607 (2012).
[18] M. Crosta, S. Trillo, and A. Fratalocchi, The Whitham approach to dispersive shocks in systems with cubic-quintic nonlinearities, New J. Phys. **14**, 093019 (2012).
[19] H. Al-Jibbouri, I. Vidanovic, A. Balaz, and A. Pelster, Geometric resonances in Bose–Einstein condensates with two- and three-body interactions, J. Phys. B **46**, 065303 (2013).
[20] R. Killip, T. Oh, O. Pocovnicu, and M. Visan, Solitons and scattering for the cubic-quintic nonlinear Schrodinger equation on R^3, Arch. Ration. Mech. Anal. **225**, 469 (2017).
[21] K. G. Zloshchastiev, Stability and Metastability of Trapless Bose-Einstein Condensates and Quantum Liquids, Z. Naturforsch. A **72**, 677 (2017).
[22] A. Bulgac, Dilute Quantum Droplets, Phys. Rev. Lett. **89**, 050402 (2002).
[23] P. M. A. Mestrom, V. E. Colussi, T. Secker, G. P. Groeneveld, and S. J. J. M. F. Kokkelmans, van der Waals Universality near a Quantum Tricritical Point, Phys. Rev. Lett. **124**, 143401 (2020).
[24] S. Tan, Three-boson problem at low energy and implications for dilute Bose-Einstein condensates, Phys. Rev. A **78**, 013636 (2008).
[25] S. Zhu and S. Tan, Three-body scattering hypervolumes of particles with short-range interactions, arXiv:1710.04147.
[26] P. M. A. Mestrom, V. E. Colussi, T. Secker, and S. J. J. M. F. Kokkelmans, Scattering hypervolume for ultracold bosons from weak to strong interactions, Phys. Rev. A **100**, 050702(R) (2019).
[27] J. P. D'Incao, Few-body physics in resonantly interacting ultracold quantum gases, J. Phys. B **51**, 043001 (2018).
[28] W. Zwerger, Quantum-unbinding near a zero temperature liquid-gas transition, J. Stat. Mech. (2019) 103104.
[29] Z. Shotan, O. Machtey, S. Kokkelmans, and L. Khaykovich, Three-Body Recombination at Vanishing Scattering Lengths in an Ultracold Bose Gas, Phys. Rev. Lett. **113**, 053202 (2014).
[30] T. Kraemer, M. Mark, P. Waldburger, J. G. Danzl, C. Chin, B. Engeser, A. D. Lange, K. Pilch, A. Jaakkola, H.-C. Nägerl, and R. Grimm, Evidence for Efimov quantum states

in an ultracold gas of caesium atoms, Nature (London) **440**, 315 (2006).
[31] P. Naidon and S. Endo, Efimov physics: A review, Rep. Prog. Phys. **80**, 056001 (2017).
[32] A. J. Daley, J. M. Taylor, S. Diehl, M. Baranov, and P. Zoller, Atomic Three-Body Loss as a Dynamical Three-Body Interaction, Phys. Rev. Lett. **102**, 040402 (2009).
[33] M. J. Mark, S. Flannigan, F. Meinert, J. P. D'Incao, A. J. Daley, and H.-C. Nägerl, Interplay between coherent and dissipative dynamics of bosonic doublons in an optical lattice, Phys. Rev. Research **2**, 043050 (2020).
[34] D. S. Petrov, Elastic multibody interactions on a lattice, Phys. Rev. A **90**, 021601(R) (2014).
[35] A. Muryshev, G. V. Shlyapnikov, W. Ertmer, K. Sengstock, and M. Lewenstein, Dynamics of Dark Solitons in Elongated Bose- Einstein Condensates, Phys. Rev. Lett. **89**, 110401 (2002).
[36] I. E. Mazets, T. Schumm, and J. Schmiedmayer, Breakdown of Integrability in a Quasi-1D Ultracold Bosonic Gas, Phys. Rev. Lett. **100**, 210403 (2008).
[37] K. Merloti, R. Dubessy, L. Longchambon, M. Olshanii, and H. Perrin, Breakdown of scale invariance in a quasi-two-dimensional Bose gas due to the presence of the third dimension, Phys. Rev. A **88**, 061603(R) (2013).
[38] C. P. Search and P. R. Berman, Manipulating the speed of sound in a two-component Bose-Einstein condensate, Phys. Rev. A **63**, 043612 (2001).
[39] J. Sanz, A. Frölian, C. S. Chisholm, C. R. Cabrera, and L. Tarruell, Interaction Control and Bright Solitons in Coherently-Coupled Bose-Einstein Condensates, Phys. Rev. Lett. **128**, 013201 (2022).
[40] The same differential mean-field shift is at the origin of the blockade of internal Josephson oscillations [41].
[41] T. Zibold, E. Nicklas, C. Gross, and M. K. Oberthaler, Classical Bifurcation at the Transition from Rabi to Josephson Dynamics, Phys. Rev. Lett. **105**, 204101 (2010).
[42] D. S. Petrov, Three-Body Interacting Bosons in Free Space, Phys. Rev. Lett. **112**, 103201 (2014).
[43] L. Lavoine, A. Hammond, A. Recati, D. Petrov, and T. Bourdel, Beyond-Mean-Field Effects in Rabi-Coupled Two-Component Bose-Einstein Condensate, Phys. Rev. Lett. **127**, 203402 (2021).
[44] We have checked that the slight imbalance between $a_{\uparrow\uparrow}$ and $a_{\downarrow\downarrow}$ does not quantitatively play a role in our experimental findings and we simply consider the average value in the analysis.
[45] E. Tiemann, P. Gersema, K. K. Voges, T. Hartmann, A. Zenesini, and S. Ospelkaus, Beyond Born-Oppenheimer approximation in ultracold atomic collisions, Phys. Rev. Research **2**, 013366 (2020).
[46] P. Cheiney, C. R. Cabrera, J. Sanz, B. Naylor, L. Tanzi, and L. Tarruell, Bright Soliton to Quantum Droplet Transition in a Mixture of Bose-Einstein Condensates, Phys. Rev. Lett. **120**, 135301 (2018).
[47] Actually, we adjust the longitudinal trapping frequency after the rf sweep in order to detect no longitudinal dynamics.
[48] We have reduced the oscillation amplitude by applying a longer rf sweep and found no change in the breathing mode frequency.
[49] Y. Kagan, E. L. Surkov, and G. V. Shlyapnikov, Evolution of a Bose-condensed gas under variations of the confining potential, Phys. Rev. A **54**, R1753 (1996).
[50] L. P. Pitaevskii and A. Rosch, Breathing modes and hidden symmetry of trapped atoms in two dimensions, Phys. Rev. A **55**, R853 (1997).
[51] F. Chevy, V. Bretin, P. Rosenbusch, K. W. Madison, and J. Dalibard, Transverse Breathing Mode of an Elongated Bose-Einstein Condensate, Phys. Rev. Lett. **88**, 250402 (2002).
[52] C. Pethick and H. Smith, *Bose–Einstein Condensation in Dilute Gases* (Cambridge University Press, Cambridge, England, 2008).
[53] N. B. Jørgensen, G. M. Bruun, and J. J. Arlt, Dilute Fluid Governed by Quantum Fluctuations, Phys. Rev. Lett. **121**, 173403 (2018).
[54] X. Antoine and R. Duboscq, GPELab, a Matlab toolbox to solve Gross-Pitaevskii equations I: Computation of stationary solutions, Comput. Phys. Commun. **185**, 2969 (2014).
[55] We have checked that the energy associated with the gradient of θ [56] adds a negligible kinetic energy in our experimental configuration. This finding justifies our local density approximation in the calculation of the internal state.
[56] M. R. Matthews, B. P. Anderson, P. C. Haljan, D. S. Hall, M. J. Holland, J. E. Williams, C. E. Wieman, and E. A. Cornell, Watching a Superfluid Untwist Itself: Recurrence of Rabi Oscillations in a Bose-Einstein Condensate, Phys. Rev. Lett. **83**, 3358 (1999).
[57] $E_{\rm int} = \int \min_\theta (E_{MF}/N) n(\mathbf{r}) \mathrm{d}^3\mathbf{r} - N\epsilon_-$, where E_{MF}/N is defined in Eq. (1).
[58] Strictly, higher order beyond mean-field corrections will make $V(s)$ increase at low s and prevent the collapse. However, this would occur at such high densities that losses would occur anyway before reaching such a small size, leaving our conclusion unchanged.
[59] R. P. Smith, R. L. D. Campbell, N. Tammuz, and Z. Hadzibabic, Effects of Interactions on the Critical Temperature of a Trapped Bose Gas, Phys. Rev. Lett. **106**, 250403 (2011).
[60] T. Mithun, K. Porsezian, and B. Dey, Vortex dynamics in cubic-quintic Bose-Einstein condensates, Phys. Rev. E **88**, 012904 (2013).
[61] Y. Kivshar and G. Agrawal, *Optical Solitons* (Academic Press, San Diego 2003).
[62] At the mean-field level, this solution is a stable fixed point of the internal state dynamics for $\gamma < 1$ [41].
[63] D. S. Petrov, Quantum Mechanical Stabilization of a Collapsing Bose-Bose Mixture, Phys. Rev. Lett. **115**, 155302 (2015).
[64] I. Ferrier-Barbut, H. Kadau, M. Schmitt, M. Wenzel, and T. Pfau, Observation of Quantum Droplets in a Strongly Dipolar Bose Gas, Phys. Rev. Lett. **116**, 215301 (2016).
[65] L. Chomaz, S. Baier, D. Petter, M. J. Mark, F. Wächtler, L. Santos, and F. Ferlaino, Quantum-Fluctuation-Driven Crossover from a Dilute Bose-Einstein Condensate to a Macrodroplet in a Dipolar Quantum Fluid, Phys. Rev. X **6**, 041039 (2016).

[66] C. R. Cabrera, L. Tanzi, J. Sanz, B. Naylor, P. Thomas, P. Cheiney, and L. Tarruell, Quantum liquid droplets in a mixture of Bose-Einstein condensates, Science **359**, 301 (2018).

[67] G. Semeghini, G. Ferioli, L. Masi, C. Mazzinghi, L. Wolswijk, F. Minardi, M. Modugno, G. Modugno, M. Inguscio, and M. Fattori, Self-Bound Quantum Droplets of Atomic Mixtures in Free Space, Phys. Rev. Lett. **120**, 235301 (2018).

[68] Z. Guo, F. Jia, L. Li, Y. Ma, J. M. Hutson, X. Cui, and D. Wang, Lee-Huang-Yang effects in the ultracold mixture of ^{23}Na and ^{87}Rb with attractive interspecies interactions, Phys. Rev. Research **3**, 033247 (2021).

[69] Y. Sekino and Y. Nishida, Quantum droplet of one-dimensional bosons with a three-body attraction, Phys. Rev. A **97**, 011602(R) (2018).

[70] Y. Nishida, Universal bound states of one-dimensional bosons with two- and three-body attractions, Phys. Rev. A **97**, 061603(R) (2018).

[71] G. Guijarro, A. Pricoupenko, G. E. Astrakharchik, J. Boronat, and D. S. Petrov, One-dimensional three-boson problem with two- and three-body interactions, Phys. Rev. A **97**, 061605(R) (2018).

[72] H. Hu, Z.-Q. Yu, J. Wang, and X.-J. Liu, First-order Bose-Einstein condensation with three-body interacting bosons, Phys. Rev. A **104**, 043301 (2021).